

Magnetization jump in one dimensional $J - Q$ model with anisotropic exchange

Bin-Bin Mao,^{1,*} Chen Cheng,^{2,†} Fu-Zhou Chen,¹ and Hong-Gang Luo^{1,2,‡}

¹*Center of Interdisciplinary Studies & Key Laboratory for Magnetism and Magnetic Materials of the Ministry of Education, Lanzhou University, Lanzhou 730000, China*

²*Beijing Computational Science Research Center, Beijing 100193, China*

We investigate the adiabatic magnetization process of the one-dimensional $J - Q$ model with XXZ anisotropy g in an external magnetic field h by using density matrix renormalization group method. According to the shape of the magnetization curves, we draw a magnetization phase diagram consisting of four phases. For a fixed nonzero pair coupling Q , i) when $g < -1$, the ground state is always ferromagnetic in spite of h ; ii) when $g > -1$ but still small, the whole magnetization curve is continuous and smooth; iii) if further increasing g , there is a macroscopic magnetization jump from partially- to fully-polarized state; iv) for a sufficiently large g , the magnetization jump is from non- to the fully-polarized state. By examining the energy per magnon and the correlation function, we find that the reason of the magnetization jump is the condensation of magnons and the formation of magnetic domains.

I. INTRODUCTION

Quantum spin systems play a very important role in condensed matter physics, because of its underlying rich physics, such as the spin liquid state [1] and the valence-bond solid (VBS) state [2]. Typically, when subjected to the external magnetic field, the magnetization process of the spin systems can also exhibit anomalous phenomena. Among them two kinds of discontinuous of the magnetization curves have attracted many interests and studies. One is the magnetization plateau, which usually accompanies with the spin excitation gap and has been found in many systems, such as the frustrated spin systems [3, 4], and quasi-periodic systems with non-trivial topological property [5, 6]. The other is the magnetization jump, which exhibits the discontinuous in the magnetization density.

The magnetization jump was first proposed by Néel [7] for the system with the Ising-like anisotropic exchange interaction, and then confirmed experimentally with hydrated copper compound [8]. Since that, in experiment, the magnetization jumps have been found in many different kinds of magnetic materials [9–16], and were also theoretically investigated in various of lattice spin systems of different dimensions [17–27]. While the reason or origin of the magnetization jumps are different, such as the magnetic domain reorientation [9, 10, 16], the spin-flop transition [18, 26, 28], the formation of bound magnon pairs [21], and the macroscopically large degeneracy at the critical value of the external magnetic field [20, 29], most of these model systems involves anisotropy or frustration.

Recently, this field driven phase transition has also been proposed in one-dimensional $J - Q$ model [30], which is first introduced by Sandvik [31] to construct a spin valence-bond-solid (VBS) state without frustration. In the presence of external magnetic field, they

demonstrate that the magnetization curve of the model displays a sharp jump from a finite to the saturated magnetization at some critical magnetic field, by numerically employing the exact diagonalization and the stochastic series expansion quantum monte carlo method [32]. The mechanism is claimed to be the onset of attractive interactions between magnons, according to the analytical results for two magnons on a ferromagnetic background. One key interesting point of their work is the existence of the magnetization jump without any anisotropy or frustration, which are the most important elements for the magnetization jump in many other systems. Due to this particularity, in the present work, we are interested in the essential physics of the magnetization jump in this model, as well as the effect of the anisotropy on the magnetization curves. In practice, we numerically investigate the zero temperature magnetization process, and obtain the magnetization phase diagram of the one-dimensional $J - Q$ model with the XXZ anisotropy. More importantly, by analyzing the average energy and the correlation function, we demonstrate that an N -magnon state with magnetic domains cannot be the ground state of the system in the grand-canonical ensemble. In other words, the formation of the magnetic domain is the reason for the magnetization jump.

The rest of the paper is organized as follows. In Sec. II, we introduce the model Hamiltonian and the numerical method. In Sec. III, we show the adiabatic magnetization curves at zero temperature and summarize the main results in a magnetization phase diagram. Sec. IV discusses the essential physics of the macroscopic magnetization jump, by analyzing the energy and the correlation function. Sec. V is the summary.

II. MODEL HAMILTONIAN AND NUMERICAL METHOD

The anisotropic $J - Q$ model in the presence of an external magnetic field is described by the Hamiltonian

$$H = -J \sum_i P_{i,i+1} - Q \sum_i P_{i,i+1} P_{i+2,i+3} - h \sum_i S_i^z, \quad (1)$$

* maobb08@lzu.edu.cn

† chengchen@csrc.ac.cn

‡ luohg@lzu.edu.cn

where $P_{i,j} \equiv \frac{1}{4} - (S_i^x S_j^x + S_i^y S_j^y + g S_i^z S_j^z)$ and g is the XXZ anisotropy. J is the Heisenberg exchange constant, Q is the coupling strength of the nearest pairs, and h is the strength of the external magnetic field. In the isotropic limit $g = 1$ and without magnetic field, the competition between J and Q terms leads to a ground state phase transition from Heisenberg ground state to the doubly degenerate VBS phase [33]. In this paper, we are more interested in the magnetization properties of the system subjected to the external magnetic field. Specially, we investigate the adiabatic magnetization process of the one-dimensional system and define the magnetization density as

$$m = \frac{2}{L} \sum_i \langle S_i^z \rangle, \quad (2)$$

where L is the system size. When $h = 0$, the ground state of the system has zero magnetization for any $g > -1$. In contrast, if h is sufficiently large, the Hamiltonian (1) has a ferromagnetic ground state with the saturated magnetization $m = 1$. The magnetization density as a function of external field h , i.e., the magnetization curve, may exhibit differently for different parameters Q and g . According to the different shapes of the magnetization curve, we can define several different magnetization phases.

In practice, we numerically employ the density matrix renormalization group (DMRG) method [34, 35], which is extremely powerful for the one dimensional systems. We perform the calculation for systems with different lattice sizes up to 240, to obtain the physics in the thermodynamic limit. The periodic boundary condition (PBC) is adopted and the DMRG many-body states are kept dynamically [36] in order to control the truncation error, which is less than 10^{-8} in the whole calculations we performed. In the whole paper, we use $J = 1$ as the energy scale and restrict Q and h to positive values.

III. MACROSCOPIC MAGNETIZATION JUMPS

A. isotropic system

We first review the magnetization property of the system in the isotropic limit, by displaying the variation of the magnetization density m in the magnetic process, as shown in Fig. 1. When $Q = 0$, the system is the spin-1/2 Heisenberg chain, and its zero temperature magnetization curve is continuous and smooth. Here the microscopic jumps and plateaus come from the finite size effect and will disappear in the thermodynamic limit. For a small $Q = 0.2$, comparing to $Q = 0$, m changes faster near the saturated magnetization, but still, goes smoothly to $m = 1$ at the same saturated field h_{sat} without a magnetization jump. However, if further increasing Q to 0.4, the magnetization density m changes suddenly from a partially polarized value m_c to $m = 1$, and the

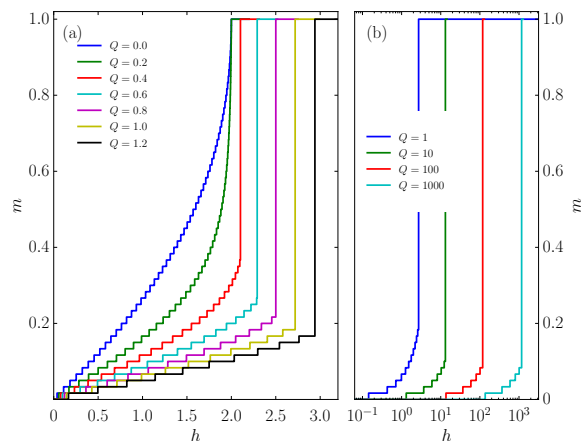


FIG. 1. (Color online) Magnetization density m as a function of external field h for different coupling Q in the isotropic case with $g = 1$. The system size $L = 120$.

saturated field h_{sat} is also larger than that for the smooth magnetization curves. This sharp jump of the magnetization curve indicates a ground state phase transition induced by the external field.

In the presence of a magnetization jump, the critical field h_{sat} increases as the coupling strength Q increases, and the critical magnetization m_c is smaller for a larger Q . However, as shown in Fig. 1(b), when Q is sufficiently large, m_c does not decrease anymore and converges to a nonzero value. There implies no direct magnetization jump from $m = 0$ to $m = 1$ even when $Q \rightarrow \infty$.

B. anisotropic system

Then we extend our investigation to the general case with a tunable anisotropy g , which can be both positive and negative. When $g < -1$, the system has a doubly degenerate ferromagnetic ground state in the absence of h , independent of the coupling strength Q . In this case, the magnetization density of the system remains the same value $m = 1$ for any positive h .

In Fig. 2, we show the magnetization curves for a fixed $Q = 1.5$ and several different anisotropy g . When $g = -0.5$, the magnetization density m increases gradually from 0 to 1 without magnetization jump. For larger values of anisotropy $g = 0.5$ and 2.0 , we can observe the shape jumps from a finite m_c to the saturated magnetization density. Furthermore, when g is sufficiently large ($g = 4.0$), there occurs a direct jump from $m = 0$ to the fully polarized state. This novel phenomenon cannot be observed in the isotropic system.

According to the different behaviors of the magnetization process, we can summarize our main results as a magnetization phase diagram consisting of four regions, as shown in Fig. 3. First, when $g < -1$, the system is in the ferromagnetic (FM) phase, and the magnetization property is trivial. When $g > -1$, the magnetiza-

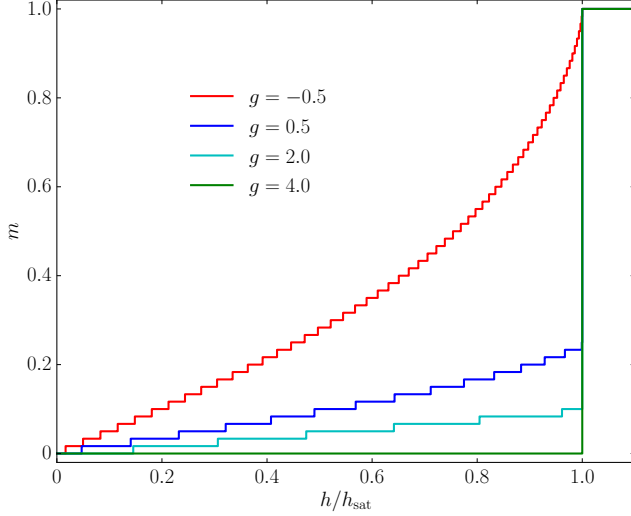


FIG. 2. (Color online) Magnetization curves for $Q = 1.5$ and different g . Here h_{sat} is the critical field when the magnetization density m goes to its saturated value. The system size $L = 120$, and the anisotropy $g = -0.5, 0.5, 2.0$, and 4.0 from left to right.

tion curve of the system has three different shapes: there is i) no magnetization jump (N-MJ), ii) a partially- to fully-polarized magnetization jump (PF-MJ), iii) a non-polarized to fully-polarized magnetization jump (NF-MJ). The phase boundaries obtained by DMRG show a convergence as the system size increases, indicating that these phases are stable in the thermodynamic limit. From these boundaries, we see that both the pair coupling Q and the anisotropy $g > -1$ can enhance the magnetization jump. Moreover, the critical anisotropy g for both boundaries seems to converge in the large Q limit.

IV. PHYSICS OF THE JUMP

A. Two-magnon state

Macroscopic magnetization jumps have been found in various of systems for different origin reasons. For the isotropic $J-Q$ model, the origin of the jump was claimed to be the attractive interaction between magnons [30]. In this subsection, we study the anisotropic model in a similar way, by comparing the energy of one- and two-magnon states on a ferromagnetic background.

We denote the ferromagnetic state as $|0\rangle = |\uparrow\uparrow\uparrow\cdots\rangle$, which is a zero-magnon state. Consider the system described by the Hamiltonian in Eq. (1), with size L and PBC, the energy of this zero-magnon state neglecting the contribution of the external field is:

$$E(0) = -J \frac{(1-g)}{4} L - Q \frac{(1-g)^2}{16} L \quad (3)$$

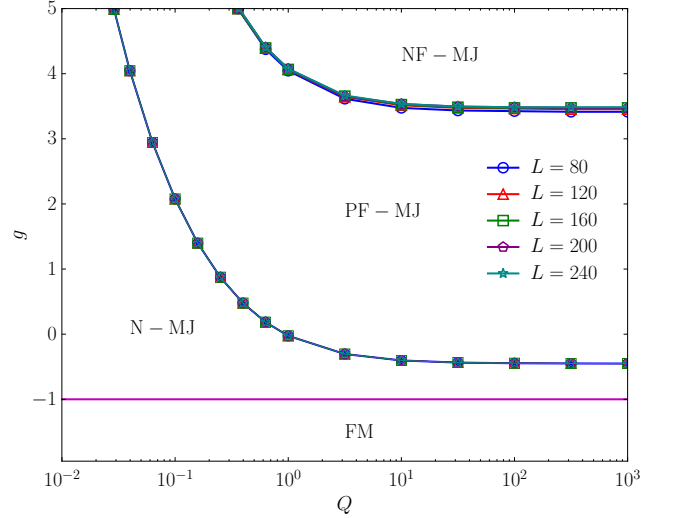


FIG. 3. (Color online) Magnetization phase diagram consisting of four phases according to the shapes of the magnetization curves: i) the ferromagnetic (FM) phase; ii) the no magnetization jump (N-MJ) phase; iii) the partially- to fully-polarized magnetization jump (PF-MJ) phase; iv) the non- to fully-polarized magnetization jump (NF-MJ) phase.

One-magnon state can be obtained by flipping a single spin of the magnon-vacuum state $|0\rangle$. Since the system is translational invariant and the position of the down spin is not important, this state can be represented as $|1\rangle = |\downarrow\uparrow\uparrow\cdots\rangle$. We can easily obtain the energy of the one-magnon state in the momentum space by Fourier transformation:

$$E_k(1) = \left[J + \frac{Q}{2} (1-g) \right] \cos(k) - Jg + \frac{Q(-g+g^2)}{2} - J \frac{(1-g)}{4} L - Q \frac{(1-g)^2}{16} L. \quad (4)$$

Notice that J and Q are both positive, then the minimum energy cost of the one-spin flipping operation defined as $\tilde{E}(1) = E(1) - E(0)$ reads

$$\tilde{E}(1) = \begin{cases} -J(1+g) - \frac{Q(1-g^2)}{2} & \text{if } g < \frac{2J}{Q} + 1, \\ J(1-g) + \frac{Q(1-g)^2}{2} & \text{if } g > \frac{2J}{Q} + 1. \end{cases} \quad (5)$$

Here $\tilde{E}(1)$ can also be considered as the energy of a free magnon. For the two-magnon case, a convenient complete basis set is made up of the two-magnon states with different distance d between two spin-down sites:

$$\begin{aligned} |2\rangle_{d=1} &= |\downarrow\downarrow\uparrow\uparrow\uparrow\cdots\rangle \\ |2\rangle_{d=2} &= |\downarrow\uparrow\downarrow\uparrow\uparrow\cdots\rangle \\ |2\rangle_{d=3} &= |\downarrow\uparrow\uparrow\downarrow\uparrow\cdots\rangle \\ &\vdots \\ |2\rangle_{d=L-1} &= |\downarrow\uparrow\uparrow\uparrow\cdots\downarrow\rangle \end{aligned} \quad (6)$$

Note that the states $|2\rangle_{d=L-1}$, $|2\rangle_{d=L-2}$ and $|2\rangle_{d=L-3}$ are equivalent to $|2\rangle_{d=1}$, $|2\rangle_{d=2}$ and $|2\rangle_{d=3}$, respectively, because of the translational invariance of the system. Acting the Hamiltonian (1) to the basis, one can get the nonzero matrix elements of the two-magnon states. For the J term, we have:

$$H_J|2\rangle_{d=1} = -J \left[\frac{(1-g)}{4}L + g \right] |2\rangle_{d=1} - J|2\rangle_{d=2} \quad (7a)$$

$$H_J|2\rangle_{d>1} = -J \left[\frac{(1-g)}{4}L + 2g \right] |2\rangle_d - J|2\rangle_{d-1} - J|2\rangle_{d+1} \quad (7b)$$

and for the Q term:

$$H_Q|2\rangle_{d=1} = Q \left[-\frac{(1-g)^2}{16}L + \frac{g^2-2g}{4} \right] |2\rangle_{d=1} - \frac{Q}{2}|2\rangle_{d=2} - \frac{Q}{4}|2\rangle_{d=3} \quad (8a)$$

$$H_Q|2\rangle_{d=2} = Q \left[-\frac{(1-g)^2}{16}L + \frac{g^2-2g-1}{2} \right] |2\rangle_{d=2} - \frac{Q}{2}|2\rangle_{d=1} - \frac{Q}{2}|2\rangle_{d=3} \quad (8b)$$

$$H_Q|2\rangle_{d=3} = Q \left[-\frac{(1-g)^2}{16}L + \frac{3g^2-4g}{4} \right] |2\rangle_{d=3} - \frac{Q(1-g)}{2}|2\rangle_{d=4} - \frac{Q}{2}|2\rangle_{d=2} - \frac{Q}{4}|2\rangle_{d=1} \quad (8c)$$

$$H_Q|2\rangle_{d>3} = Q \left[-\frac{(1-g)^2}{16}L + (g^2-g) \right] |2\rangle_d - \frac{Q}{2}(1-g)|2\rangle_{d-1} - \frac{Q}{2}(1-g)|2\rangle_{d+1} \quad (8d)$$

We use $\tilde{E}(2) = E(2) - E(0)$ denoting the minimum energy cost for the 2-spin flipping operation from the magnon-vacuum state, which is the ground state energy of the matrix $\tilde{H}(2) = H_J + H_Q - E(0)$ in the two-magnon basis. Here $\tilde{H}(2)$ reads

$$\tilde{H}(2) = \begin{pmatrix} Q\frac{g^2-2g}{4} - Jg & -\frac{Q}{2} - J & -\frac{Q}{4} \\ -\frac{Q}{2} - J & Q\frac{g^2-2g-1}{2} - 2Jg & -\frac{Q}{2} - J \\ -\frac{Q}{4} & -\frac{Q}{2} - J & Q\frac{3g^2-4g}{4} - 2Jg \\ & & -\frac{Q(1-g)}{2} - J & Q(g^2-g) - 2Jg \\ & & & \ddots \end{pmatrix} \quad (9)$$

Then we can compare the energy of the one- and two-magnon excitations by measuring $\tilde{E}(2) - 2\tilde{E}(1)$, in order to get a clue of the magnetization jump in the few magnon limit. The negative value of $\tilde{E}(2) - 2\tilde{E}(1)$ indicates the effective attractive interaction between the two magnons, and the magnetization curve exhibits a macroscopic magnetization jump near the saturated magnetization. In contrast, if $\tilde{E}(2) - 2\tilde{E}(1) > 0$, the effective interaction is repulsive and there is no signal of a magnetization jump at least for the few magnon limit. $\tilde{E}(2) - 2\tilde{E}(1) = 0$ is the critical case, and the system is in the noninteracting magnon ground state.

In Fig. 4(a) we plot $\tilde{E}(2) - 2\tilde{E}(1)$ for $L = 128$ and several different Q . The magnetization curve is smooth and continuous when the pair coupling $Q = 0$. Correspondingly, in this case $\tilde{E}(2) - 2\tilde{E}(1)$ is almost independent of g and always positive. However, for a very small $Q = 0.05$, $\tilde{E}(2) - 2\tilde{E}(1)$ is positive for small values of g , but negative when g is large enough. As one increases the anisotropy g , the effective interaction between magnons changes from repulsive to attractive. This is the derivation of the magnetization jump, induced by

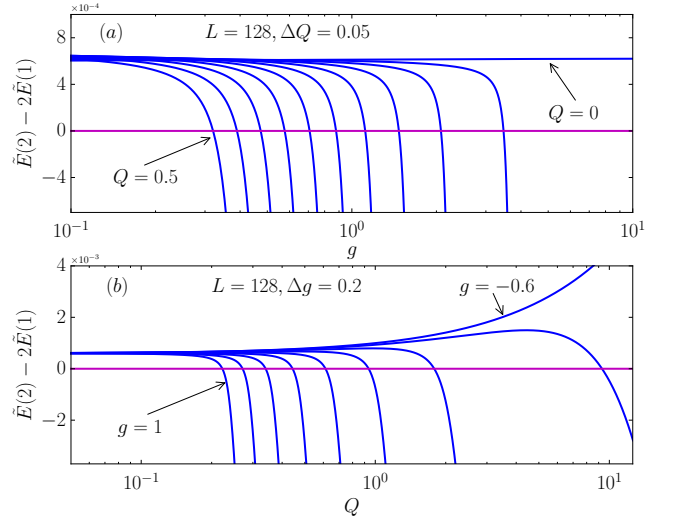


FIG. 4. (Color online) $\tilde{E}(2) - 2\tilde{E}(1)$ as a function of (a) g for different Q , (b) Q for different g . The system size $L = 128$.

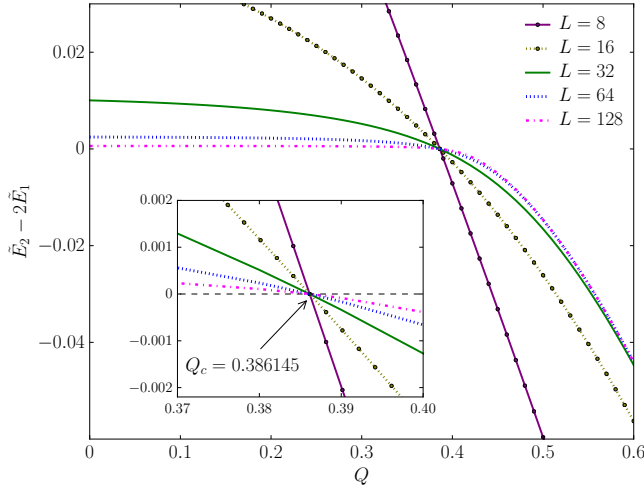


FIG. 5. (Color online) $\tilde{E}(2) - 2\tilde{E}(1)$ as a function of Q for $g = 0.5$ and different L . The black dashed line in inset is for $\tilde{E}(2) - 2\tilde{E}(1) = 0$.

the anisotropy. The boundary between the N-MJ phase and the PF-MJ phase in Fig. 3 can be determined by the critical g when $\tilde{E}(2) - 2\tilde{E}(1) = 0$. From the curves for different Q , we can also conclude that the necessary g for a magnetization jump is smaller when Q is larger, in agreement with the results by DMRG.

Similar to Fig. 4(a), we show $\tilde{E}(2) - 2\tilde{E}(1)$ as a function of Q for different g in Fig 4(b). In the isotropic case with $g = 1$, $\tilde{E}(2) - 2\tilde{E}(1) > 0$ for smaller Q , but becomes negative for larger Q . A magnetization phase transition from the N-MJ phase to the PF-MJ phase occurs at the critical $Q_c(g = 1) = 2/9$, in agreement with the result in Ref. [30]. Different curves for decreased g show that the magnetization jump exists in the anisotropic case, and the critical value of Q is larger as for smaller g . However, when g is too small ($g = -0.6$), the curve of $\tilde{E}(2) - 2\tilde{E}(1)$ goes up as Q increases, and there is no cross with $\tilde{E}(2) - 2\tilde{E}(1) = 0$. In this case, the interaction between the two magnons is always repulsive, and there is no magnetization jump near the saturated magnetization.

In order to see the finite size effect in the few magnon limit, we plot $\tilde{E}(2) - 2\tilde{E}(1)$ for $g = 0.5$ as a function of Q for different system sizes, as shown in Fig. 5. All these curves have a precise cross at $\tilde{E}(2) - 2\tilde{E}(1) = 0$ and a critical $Q_c(g = 0.5) = 0.386145$ even for $L = 8$, which is the minimum system size to include all the information of the effective Hamiltonian described by Eq. (9). Therefore, the finite size effect in the few magnon limit is negligible.

We also investigate the probability $P(d)$ of the magnon distance d in the two-magnon ground state. As shown in Fig. 6, for the small pair couplings ($Q = 0, 0.2$) where $\tilde{E}(2) - 2\tilde{E}(1) > 0$, $P(d)$ increases as distance d increases. It means that the two magnons tends to stay apart from each other as they feel effective long-range re-

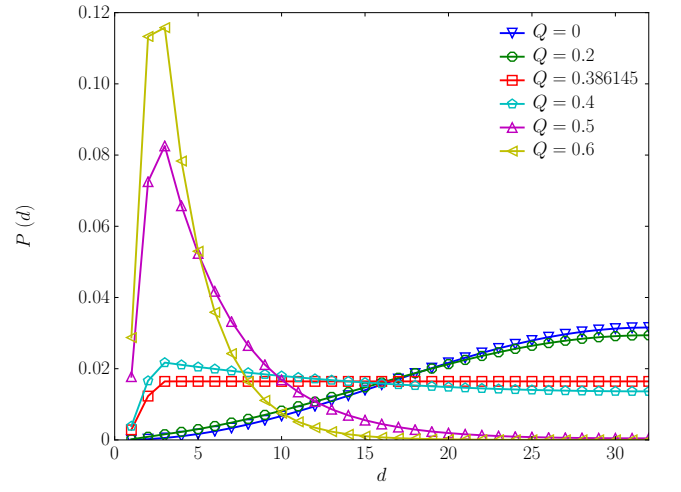


FIG. 6. (Color online) Probability $P(d)$ of the distance d between two magnons for $g = 0.5$, $L = 64$ and different Q .

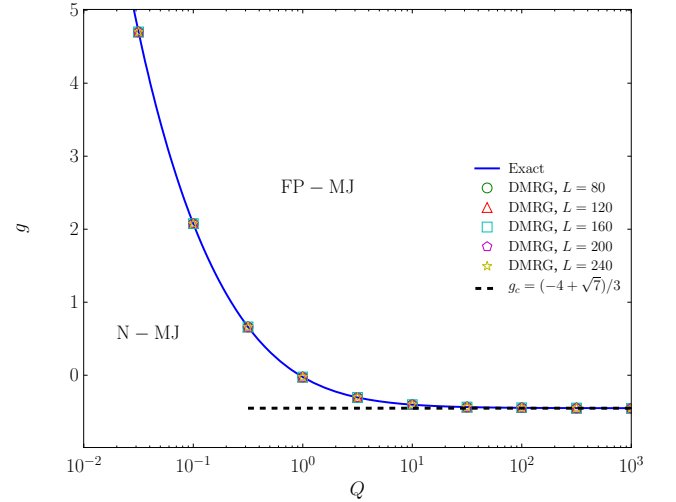


FIG. 7. (Color online) Phase boundary between the N-MJ and PF-MJ phase. Analytical and numerical results show great consistency.

pulsive interaction. In contrast, when Q is large enough ($Q = 0.4, 0.5, 0.6$), the magnons prefer to stay closely together as having attractive interactions between them. At the critical point $Q_c(g = 0.5) = 0.386145$, there is no interaction between magnons unless they *touch* each other (for $d \leq 3$), and the probability $P(d)$ is uniform for $d > 3$.

As discussed above, the phase boundary between the N-MJ and PF-MJ phases can be exactly determined by comparing the energy of one- and two-magnon excitations. We show the analytical results in Fig. 7, which perfectly agrees with the numerical results by DMRG. We also notice the asymptotic behavior of this curve when the pair coupling Q is extremely large. At the

limit $Q \rightarrow \infty$, the one-magnon excitation energy is

$$\tilde{E}(1)/Q = -\frac{1}{2}(1 - g^2), \quad (10)$$

here we have ignored the infinite small terms proportional to $1/Q$. Similarly, ignoring the $O(1/Q)$ terms, the two-magnon excitation is described by the matrix

$$\tilde{H}(2)/Q = \begin{pmatrix} \frac{g^2-2g}{4} & -\frac{1}{2} & -\frac{1}{4} \\ -\frac{1}{2} & \frac{g^2-2g-1}{2} & -\frac{1}{2} \\ -\frac{1}{4} & -\frac{1}{2} & \frac{3g^2-4g}{2} & -\frac{1-g}{2} \\ & & -\frac{1-g}{2} & g^2-g \\ & & & \ddots \end{pmatrix}. \quad (11)$$

At the critical point with $\tilde{E}(2) - 2\tilde{E}(1) = 0$, the magnons are free and the wavefunction is uniformly distributed when $d > 3$ [see Fig. 6]. Therefore, the critical wavefunction can be assumed as

$$|G\rangle_2 = \frac{1}{N} [a|2\rangle_{d=1} + b|2\rangle_{d=2} + c|2\rangle_{d=3} + \sum_{d=4}^{L-4} |2\rangle_d + c|2\rangle_{d=L-3} + b|2\rangle_{d=L-2} + a|2\rangle_{d=L-1}]. \quad (12)$$

Applying the Hamiltonian in Eq. 11 to the wavefunction $|G\rangle_2$, we can get a set of equations. By solving them, the critical g in the $Q \rightarrow \infty$ limit can be obtained as $g_c(Q \rightarrow \infty) = (-4 + \sqrt{7})/3$, as the black dashed line shown in Fig. 7. For any anisotropy g below this value, the magnetization curve of the system is always smooth and continuous.

B. N -magnon states

The analysis of the effective interaction between magnons in the two-magnon state already gives a clue to the origin of the magnetization jump in the few-magnon limit. Furthermore, in this subsection, we explicitly investigate the magnetization process in the presence of the external field. In this case, the arbitrary N -magnon state has to be considered. The energy of the N -magnon state subjected to the external field h is

$$E(N, h) = E(N) - h\langle S_{tot}^z \rangle, \quad (13)$$

where the magnon number N is equivalent to the number of the down spins, and $\langle S_{tot}^z \rangle = \sum_i \langle S_i^z \rangle$ is equal to $L/2 - N$. For simplicity, we use $E(N)$ instead of $E(N, 0)$ here and in the following.

Consider this N -magnon state as the ground state of the system at some proper magnetic field h during the magnetization process. Then the energy $E(N, h)$ must satisfy the following relations:

$$E(N, h) < E(0, h), \quad (14)$$

$$E(N, h) < E(N+1, h). \quad (15)$$

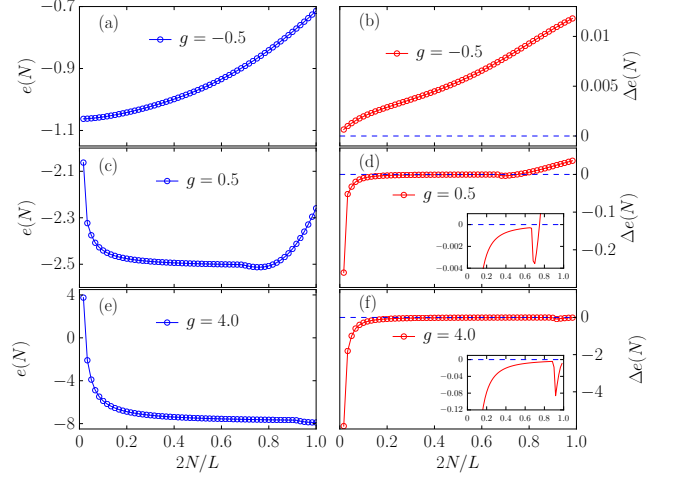


FIG. 8. (Color online) The energy per magnon $e(N)$ in (a) the N-MJ phase ($g = -0.5$), (c) the PF-MJ phase ($g = 0.5$), and (e) the NF-MJ phase ($g = 4.0$). (b), (d) and (f) are the corresponding energy difference $\Delta e(N)$ for (a), (c), and (e), respectively. For all the curves $Q = 1.5$ and $L = 120$.

By inserting Eq. (13) into Eqs. (14) and (15), one can easily obtain the necessary requirement of the external field h :

$$h < -[E(N) - E(0)]/N, \quad (16)$$

$$h > E(N) - E(N+1). \quad (17)$$

Combine Eqs. (16) and (17), one further obtains

$$e(N) < e(N+1), \quad (18)$$

where $e(N) = [E(N) - E(0)]/N$ is the the ground state energy per magnon for the N -magnon state in the absence of h . If the relationship in Eq. (18) can not be satisfied, then this N -magnon state can never be the ground state during the magnetization process. This is the origin of the macroscopic magnetization jump, from the perspective of the energy. By taking $N = 2$, one can also understand the reason why the phase boundary between the N-MJ and PF-MJ phases can be determined by comparing the excitation energies in the few magnon limit.

Fig. 8 shows the numerical results from DMRG for $Q = 1.5$ and several different g . First, in the N-MJ phase ($g = -0.5$), where the magnetization curve of the system is smooth and continuous [see Fig. 2], the energy per magnon $e(N)$ increases monotonously as the number N increases, as shown in Fig. 8(a). In this case, the energy difference $\Delta e(N) = e(N+1) - e(N)$ shown in Fig. 8(b) is always positive, i.e., Eq. (18) is always satisfied. Therefore, there is no magnetization jump. We also notice that $e(N) > e(1)$ for all these states, which means that the energy of the N -magnon state is larger than N free magnons. In this sense the effective interactions between magnons is always repulsive.

In the PF-MJ phase ($g = 0.5$), as shown in Fig. 8(c),

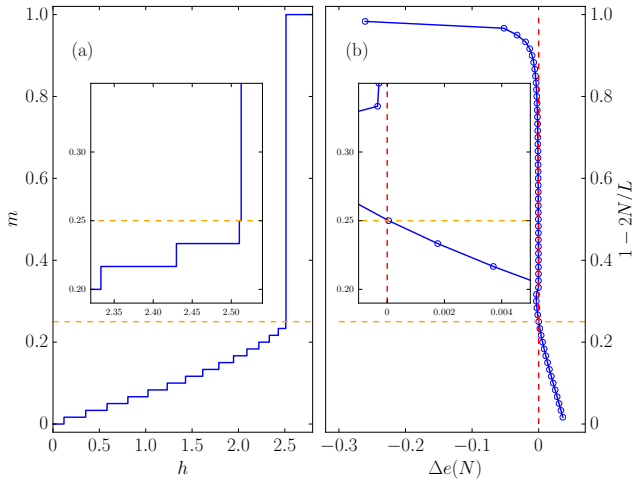


FIG. 9. (Color online) Comparison between (a) the magnetization curve and (b) the rotated plot for $\Delta e(N)$ as a function of $m = 1 - 2N/L$. The N -magnon states with positive (negative) $\Delta e(N)$ correspond to the continuous part (sharp jump) of the magnetization curve. Here $g = 0.5$, $Q = 1.5$, and $L = 120$.

as N increases, the energy per magnon $e(N)$ decreases for smaller N but increases for larger N . As shown in Fig. 8(d), there exists a region where the energy difference $\Delta e(N) < 0$, and adding a magnon to the N -magnon state will decrease the average energy of the magnons. This indicates the condensation of magnons, and the formation of the magnetic domain in these N -magnon states. These states can not be the ground state of the system in the magnetization process, and correspondingly the magnetization curve has a macroscopic jump.

Figs. 8(e) and 8(f) show the results for the NF-MJ phase ($g = 4.0$) with the magnetization jump from $m = 0$ to 1. In this phase, the energy per magnon $e(N)$ decreases monotonously as the number N increases, and the energy difference $\Delta e(N)$ is negative for arbitrary magnetization density.

We also analyze the energy per magnon in a more explicit way, by directly comparing the magnetization curve and the energy difference $\Delta e(N)$. For a magnetization curve in the PF-MJ phase, as shown in Fig. 9(a), there is a macroscopic jump from a critical m_c to $m = 1$ at the critical field h_{sat} . Since for an N -magnon state, we have $m = 1 - 2N/L$, then m_c can be precisely determined by the magnon number N where $\Delta e(N)$ is positive and $\Delta e(N - 1)$ is negative, as shown Fig. 9(b). Moreover, by considering the critical case of Eq. (16), we can also get the critical field $h_{\text{sat}} = -e(N)$.

We can retrieve the magnetization phase diagram by plotting the critical magnetization m_c in the parameter space $\{Q, g\}$, as shown in Fig. 10. When the magnetization curve is smooth and continuous, m_c should be 1 in the thermodynamic limit, indicating there is no magnetization jump. However, for the finite size system, we have

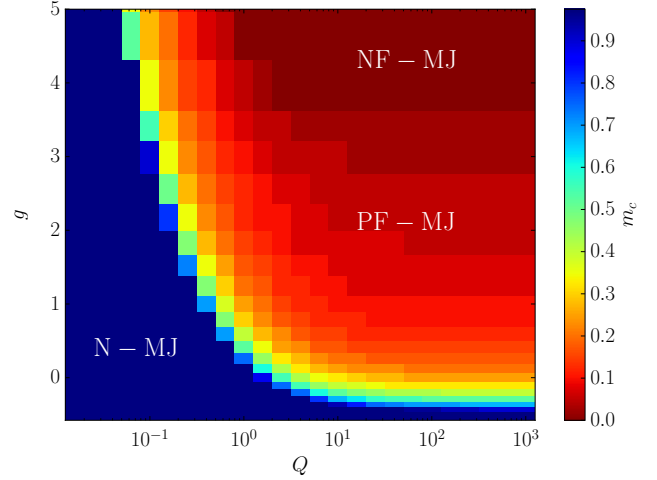


FIG. 10. (Color online) Magnetization phase diagram shown by the critical magnetization m_c in $\{Q, g\}$ space. Here we use the data for $L = 80$.

$m_c = 1 - 2/L$ because of a microscopic quantized jump. Nevertheless, the N-MJ phase denoted by the darkest blue is distinct in Fig. 10. For a fixed $g > (-4 + \sqrt{7})/3$, the magnetization jump appears as Q increases to the critical value, and m_c decreases with the increasing of Q . Finally, when g and Q are both sufficiently large, the system is in the NF-MJ phase with $m_c = 0$. All these phases and the corresponding phase boundaries are explicit and clear.

C. Correlation functions

In Sec. IV B, we study the energy of the N -magnon states, and demonstrate that some of them can never be the ground state of the system in the grand canonical ensemble. Therefore, these states are *jumped over* during the magnetization process. In this subsection, we are interested in the difference between the structures of the normal states and the *jumped over* states. To unveil the physics of the magnetization jump beyond the energy perspective, we investigate the spin-spin correlation function:

$$C_S(r) = \langle S_0^z S_r^z \rangle - \langle S_0^z \rangle \langle S_r^z \rangle. \quad (19)$$

where r is real space coordinate. The numerical results are shown in Fig. 11 for several selected N -magnon states in different phases.

First, in the N-MJ phase ($g = -0.5$), independent of the magnon number N , the spin-spin correlation $C_S(r)$ is negative for all the distance $r > 0$, and rapidly decays to 0 as r increases. In this case, a spin has anti-ferromagnetic correlation with the environment, and is screened due to the strong quantum fluctuation. The states have no long-range order (LRO) when the magnetization curve of the system is smooth and continuous.

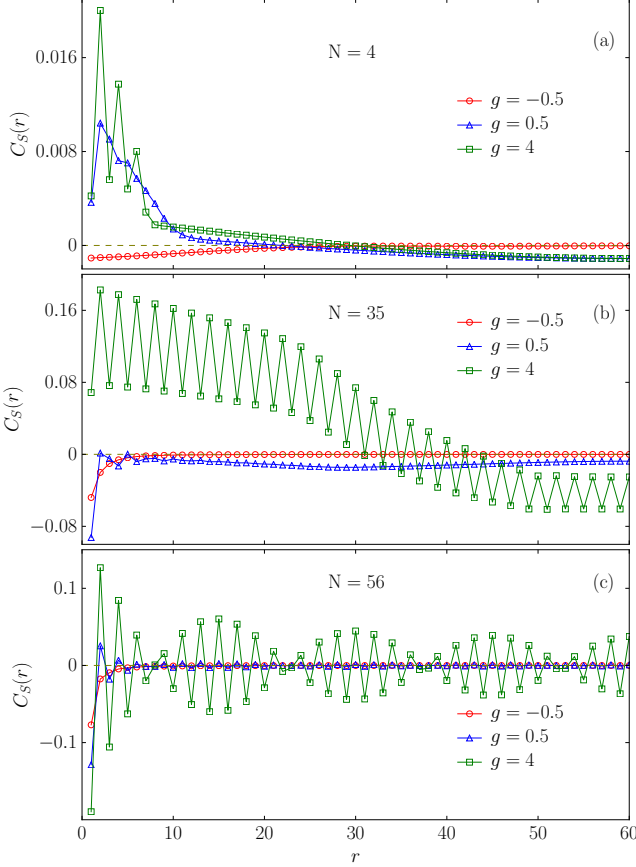


FIG. 11. (Color online) Spin-spin correlation function $C_S(r)$ for different g and N . Here $Q = 1.5$ and $L = 120$.

In the PF-MJ phase ($g = 0.5$), the magnetization curve is continuous at some magnetization density, and then has a sharp jump. The red squared-line shown in Fig. 11(a) for $N = 4$ is the correlation function of one of these *jumped over* states. In this state, $C_S(r)$ is positive when the distance r is small but negative when the spins are far apart from each other, which is the typical behavior of the system has two ferromagnetic domains. We also notice $C_S(r)$ has a finite value even when $r = L/2$, which is the largest distance possible for the finite system with system size L . In fact, $C_S(r)$ seems to converge when r is large enough. This indicates the anti-ferromagnetic (AFM) long-range order of the *jumped over* states. The AFM-LRO still can be observed when $N = 35$, as this N -magnon states still can not be the ground state in the grand canonical ensemble, as the red squared-line shown in Fig. 11(b). Further increasing the magnon number N , the correlation function $C_S(r)$ of the 56-magnon decays rapidly to zero, similar to the situation in the N-MJ phase. The AFM-LRO disappears, and the magnetization curve in this region is continuous.

The correlation functions are more complicated in the NF-MJ phase ($g = 4.0$). Since the anisotropy g is so large, the diagonal term of the Hamiltonian dominates

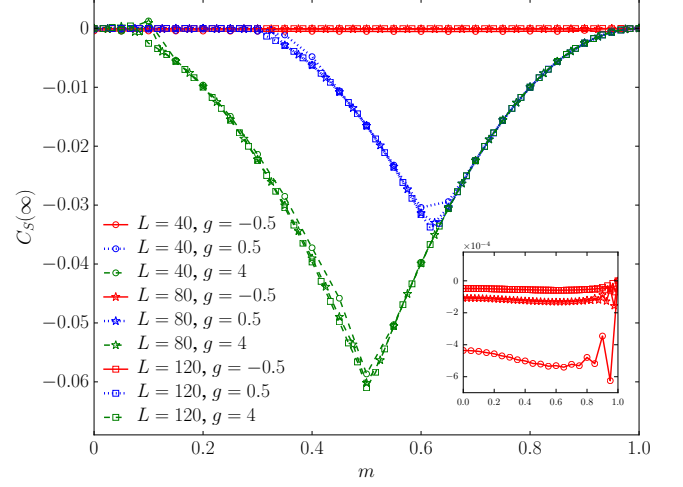


FIG. 12. (Color online) Spin-spin correlation function in the long-range limit as a function of $m = 1 - 2N/L$ for $Q = 1.5$, different anisotropy g , and different system sizes. The inset is a zoom-in for $g = -0.5$.

and the quantum effect has been partially depressed. We can observe the strong fluctuation of $C_S(r)$ at very large distance, especially when the magnon number N is large. Nevertheless, when N is small ($N = 4$ and 35), besides the fluctuations at near distance, the long-range nature of domain walls is still true at large distance. For a large $N = 56$, which is near the zero magnetization, the correlation function shown in Fig. 11(c) exhibit a classical Néel order.

We plot the long-range correlation function $C_S(\infty)$ as a function of magnetization density $m = 1 - 2N/L$ in Fig. 12. Here we define $C_S(\infty) = (C_S(L/2) + C_S(L/2 - 1))/2$ to remove the strong fluctuation when g is very large. For the N-MJ phase without magnetization jump, $C_S(\infty)$ is very small for all the magnetization densities, and its amplitude decreases as L increases [see inset]. Therefore, in the thermodynamic limit $C_S(\infty)$ is zero, and there is no LRO in this phase.

In the PF-MJ phase ($g = 0.5$), $C_S(\infty)$ approaches 0 for small magnetization densities, where the magnetization curve is continuous. For these *jumped over* states at larger m , $C_S(\infty)$ is nonzero and show convergence for different system sizes. In the thermodynamic limit, the *jumped over* states has AFM-LRO because of the formation of magnetic domains.

In the NF-MJ phase ($g = 4.0$), $C_S(\infty)$ is nonzero for larger magnetization density. Specially, for m between 0.7 and 1, $C_S(\infty)$ is the same as in the PF-MJ phase independent of the system size, as these N -magnon states share the same domain structure. However, different with the PF-MJ phase, the spin-spin correlation function has large fluctuations in the long-range limit, for these states with magnetization densities at the left of the deep. For states near $m = 0$ has nearly zero $C_S(\infty)$, there is no AFM-LRO of domains, but the spin-spin cor-

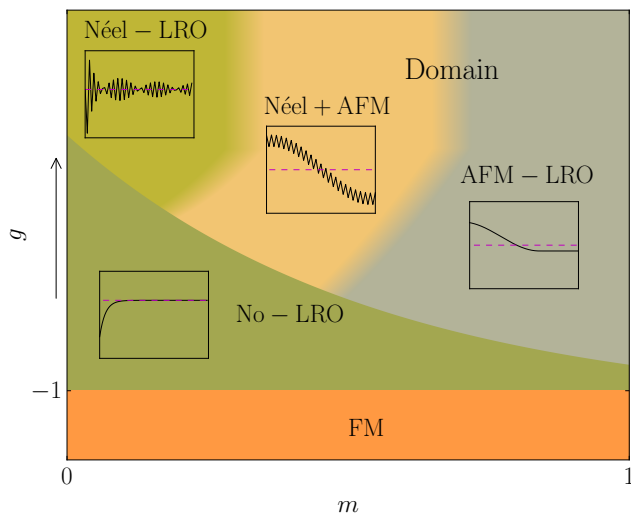


FIG. 13. (Color online) The schematic phase diagram for a fixed nonzero Q in the absence of external field h . In each inset, the black solid-line represents the schematic spin-spin correlation function $C_S(r)$, and the magenta dashed-line denotes $C_S(r) = 0$.

relation function has long-range Néel fluctuation.

V. SUMMARY AND DISCUSSION

In this work, we systematically investigate the adiabatic magnetization properties of the 1D anisotropic $J - Q$ model at zero temperature, by numerically using the DMRG method. We have found that both the pair coupling Q and the anisotropy g can enhance the magnetization jump, which indicates a field driven phase

transition. According to the shapes of the magnetization curve, we draw a magnetization phase diagram consisting of four phases: the FM phase, the N-MJ phase without magnetization jump, the PF-MJ phase with a partially-to fully- polarized magnetization jump, and specially the NF-MJ phase with a direct magnetization jump from non- to fully-polarized states, which does not exist in the isotropic $J - Q$ model.

We further study the nature of the magnetization jump, by examining the energy and structure of the N -magnon states in the absence of external field h . From the energy consideration, the origin of the jump is the condensation of magnons. By explicitly investigate the spin-spin correlation function, we confirm that the spins condensate and form the magnetic domain in these *jumped over* states. A schematic phase diagram is shown in Fig. 13 for a fixed non-zero pair coupling: i) Whenever the magnetization curve is continuous, the corresponding ground states of the system cannot have any long-range order; ii) Any states with long-range orders cannot be the ground state of the system during the magnetization process, and therefore the magnetization jump arises.

ACKNOWLEDGMENTS

The authors acknowledge useful discussions with D-X. Yao, H. Shao, W-A. Guo and L. Wang. H-G. Luo acknowledges the support from NSFC (Grants No. 11325417, 11674139) and PCSIRT (Grant No. IRT-16R35). C. Cheng acknowledges support from NSAF U1530401 and computational resource from the Beijing Computational Science Research Center.

-
- [1] P. W. Anderson, “The resonating valence bond state in La_2CuO_4 and superconductivity,” *Science* **235**, 1196–1198 (1987).
 - [2] N. Read and S. Sachdev, “Valence-bond and spin-peierls ground states of low-dimensional quantum antiferromagnets,” *Phys. Rev. Lett.* **62**, 1694–1697 (1989).
 - [3] T. Ono, H. Tanaka, K. H. Aruga, F. Ishikawa, H. Mitamura, and T. Goto, “Magnetization plateau in the frustrated quantum spin system Cs_2CuBr_4 ,” *Phys. Rev. B* **67**, 104431 (2003).
 - [4] A. Honecker, J. Schulenburg, and J. Richter, “Magnetization plateaus in frustrated antiferromagnetic quantum spin models,” *J. Phys.: Condens. Matter* **16**, S749 (2004).
 - [5] H. Kazuo, “Magnetic properties of the spin-1/2 ferromagnetic-ferromagnetic-antiferromagnetic trimerized heisenberg chain,” *J. Phys. Soc. Jpn.* **63**, 2359 (1993).
 - [6] H. P. Hu, C. Cheng, Z. H. Xu, H. G. Luo, and S. Chen, “Topological nature of magnetization plateaus in periodically modulated quantum spin chains,” *Phys. Rev. B* **90**, 035150 (2014).
 - [7] Néel., “Propriétés magnétiques de l’état magnétique et énergie d’interaction entre atomes magnétiques,” *Ann. Phys. (Paris)* **5**, 232 (1936).
 - [8] N. J. Poulis, J. van den Handel, J. Ubbink, J. A. Poulis, and C. J. Gorter, “On antiferromagnetism in a single crystal,” *Phys. Rev.* **82**, 552–552 (1951).
 - [9] H. Bjerrum Møller, S. M. Shapiro, and R. J. Birgeneau, “Field-dependent magnetic phase transitions in mixed-valent TmSe ,” *Phys. Rev. Lett.* **39**, 1021–1025 (1977).
 - [10] V. Hardy, A. Maignan, S. Hébert, C. Yaïcle, C. Martin, M. Hervieu, M. R. Lees, G. Rowlands, D. Mc K. Paul, and B. Raveau, “Observation of spontaneous magnetization jumps in manganites,” *Phys. Rev. B* **68**, 220402 (2003).
 - [11] L. Ghivelder, R. S. Freitas, M. G. das Virgens, M. A. Continentino, H. Martinho, L. Granja, M. Quintero, G. Leyva, P. Levy, and F. Parisi, “Abrupt field-induced

- transition triggered by magnetocaloric effect in phase-separated manganites,” *Phys. Rev. B* **69**, 214414 (2004).
- [12] S. Yoshii, T. Yamamoto, M. Hagiwara, T. Takeuchi, A. Shigekawa, S. Michimura, F. Iga, T. Takabatake, and K. Kindo, “High-field magnetization of TbB_4 ,” *J. Magn. Magn. Mater.* **310**, 1282 – 1284 (2007).
- [13] J. Kishine, I. G. Bostrem, A. S. Ovchinnikov, and V. E. Sinitsyn, “Topological magnetization jumps in a confined chiral soliton lattice,” *Phys. Rev. B* **89**, 014419 (2014).
- [14] L. V. B. Diop, O. Isnard, and J. Rodríguez-Carvajal, “Ultrasharp magnetization steps in the antiferromagnetic itinerant-electron system $\text{LaFe}_{12}\text{B}_6$,” *Phys. Rev. B* **93**, 014440 (2016).
- [15] M. Manago, K. Ishida, Z.Q. Mao, and Y. Maeno, “Absence of the ^{17}O knight-shift changes across the first-order phase transition line in Sr_2RuO_4 ,” *Phys. Rev. B* **94**, 180507 (2016).
- [16] B. Maji, K. G. Suresh, and A. K. Nigam, “Observation of spontaneous magnetization jump and field-induced irreversibility in Nd_5Ge_3 ,” *EPL(Europhysics Letters)* **91**, 37007 (2010).
- [17] M. Kohno and M. Takahashi, “Magnetization process of the spin-1/2 XXZ models on square and cubic lattices,” *Phys. Rev. B* **56**, 3212–3217 (1997).
- [18] T. Sakai and M. Takahashi, “Metamagnetism of antiferromagnetic XXZ quantum spin chains,” *Phys. Rev. B* **60**, 7295–7298 (1999).
- [19] A. A. Aligia, “Magnetization jump in the XXZ chain with next-nearest-neighbor exchange,” *Phys. Rev. B* **63**, 014402 (2000).
- [20] J. Schulenburg, A. Honecker, J. Schnack, J. Richter, and H.-J. Schmidt, “Macroscopic magnetization jumps due to independent magnons in frustrated quantum spin lattices,” *Phys. Rev. Lett.* **88**, 167207 (2002).
- [21] D. V. Dmitriev and V. Y. Krivnov, “Frustrated ferromagnetic spin-1/2 chain in a magnetic field,” *Phys. Rev. B* **73**, 024402 (2006).
- [22] A.V. Kalinov, L.M. Fisher, I.F. Voloshin, N.A. Babushkina, D.I. Khomskii, and T.T.M. Palstra, “Possible spin-glass state in SmSr -manganites as the origin of the magnetization jumps,” *J. Magn. Magn. Mater.* **300**, e399 – e402 (2006).
- [23] F. Heidrich-Meisner, I. P. McCulloch, and A. K. Kolezhuk, “Phase diagram of an anisotropic frustrated ferromagnetic spin-1/2 chain in a magnetic field: A density matrix renormalization group study,” *Phys. Rev. B* **80**, 144417 (2009).
- [24] A. K. Kolezhuk, F. Heidrich-Meisner, S. Greschner, and T. Vekua, “Frustrated spin chains in strong magnetic field: Dilute two-component bose gas regime,” *Phys. Rev. B* **85**, 064420 (2012).
- [25] F. A. Gómez Albarracín, M. Arlego, and H. D. Rosales, “Magnetization plateaus and jumps in a frustrated four-leg spin tube under a magnetic field,” *Phys. Rev. B* **90**, 174403 (2014).
- [26] N. Hiroki, H. Yasumasa, and S. Tôru, “Magnetization jump in the magnetization process of the spin-1/2 heisenberg antiferromagnet on a distorted square-kagome lattice,” *J. Phys. Soc. Jpn.* **84**, 114703 (2015).
- [27] K. Morita and N. Shibata, “Multiple magnetization plateaus and magnetic structures in the $s=1/2$ heisenberg model on the checkerboard lattice,” *Phys. Rev. B* **94**, 140404 (2016).
- [28] C. Gerhardt, K. H. Mütter, and H. Kröger, “Metamagnetism in the XXZ model with next-to-nearest-neighbor coupling,” *Phys. Rev. B* **57**, 11504–11509 (1998).
- [29] J. Richter, J. Schulenburg, A. Honecker, J. Schnack, and H.-J. Schmidt, “Exact eigenstates and macroscopic magnetization jumps in strongly frustrated spin lattices,” *J. Phys.: Condens. Matter* **16**, S779 (2004).
- [30] A. W. Sandvik and A. laizzi, “Field-driven quantum phase transitions in $s=1/2$ spin chains,” *ArXiv:1603.04359* (2016).
- [31] A. W. Sandvik, “Evidence for deconfined quantum criticality in a two-dimensional heisenberg model with four-spin interactions,” *Phys. Rev. Lett.* **98**, 227202 (2007).
- [32] A. W. Sandvik and J. Kurkijärvi, “Quantum monte carlo simulation method for spin systems,” *Phys. Rev. B* **43**, 5950–5961 (1991).
- [33] Y. Tang and A. W. Sandvik, “Method to characterize spinons as emergent elementary particles,” *Phys. Rev. Lett.* **107**, 157201 (2011).
- [34] S. R. White, “Density matrix formulation for quantum renormalization groups,” *Phys. Rev. Lett.* **69**, 2863–2866 (1992).
- [35] S. R. White, “Density-matrix algorithms for quantum renormalization groups,” *Phys. Rev. B* **48**, 10345–10356 (1993).
- [36] Ö. Legeza, J. Röder, and B. A. Hess, “Controlling the accuracy of the density-matrix renormalization-group method: The dynamical block state selection approach,” *Phys. Rev. B* **67**, 125114 (2003).